Journal of Biomolecular NMR, 10 (1997) 363–372
KLUWER/ESCOM

J-Bio NMR 469

Off-resonance rf fields in heteronuclear NMR: Application to the study of slow motions*

Sophie Zinn-Justin[a,**], Patrick Berthault[b], Marc Guenneugues[a] and Hervé Desvaux[b]

[a]*Département d'Ingénierie et d'Etude des Protéines, CEA Saclay, F-91191 Gif sur Yvette Cedex, France*
[b]*Service de Chimie Moléculaire, CEA Saclay, F-91191 Gif sur Yvette Cedex, France*

Received 6 January 1997
Accepted 18 June 1997

Keywords: Heteronuclear relaxation; Protein dynamics; Chemical exchange; Off-resonance field; ^{15}N NMR; Toxin

Summary

The advantages of using off-resonance rf fields in heteronuclear self-relaxation experiments are explored on a fully ^{15}N-enriched protein. It is firstly shown that *in the absence of slow motions* the longitudinal and transverse ^{15}N self-relaxation rate values derived with this method are in agreement with the ones measured by the classical inversion-recovery and Carr–Purcell–Meiboom–Gill (CPMG) sequences, respectively. Secondly, by comparing the ^{15}N transverse self-relaxation rates obtained by the proposed off-resonance sequence and by the CPMG sequence, 11 residues out of the 61 of toxin α are shown to exhibit a chemical exchange phenomenon in water on a time scale ranging from 1 μs to 100 ms. By varying the effective field amplitude, chemical exchange processes involving these residues are measured and the corresponding correlation times are evaluated without having assumed any motion model. Similar, though less precise, results are given by the analysis of the ^{15}N off-resonance self-relaxation rates on the basis of the Lipari–Szabo model to describe the fast internal dynamics of toxin α.

Introduction

NMR provides information on the molecular dynamics over a wide time range, from picoseconds to days (Wagner and Wüthrich, 1982; Wagner, 1993). In particular, ^{15}N or ^{13}C relaxation times depend essentially on the reorientational dynamics of the ^{15}NH or ^{13}CH vectors in the nanosecond time scale. However, much slower motions (with characteristic times ranging from microseconds to milliseconds) may have a non-vanishing contribution to the transverse self-relaxation. The characterization of these motions, often referred to as fast chemical exchange processes, is still a difficult task, although different methods have been proposed. The first method consists in measuring the ^{15}N transverse self-relaxation rate R_2 using a Carr-Purcell-Meiboom-Gill (CPMG) sequence (Carr and Purcell, 1954; Meiboom and Gill, 1958; see Fig. 1a). The dependence of R_2 on the CPMG delay makes it possible to evaluate chemical exchange rates in the range 10^3–10^4 Hz (Gutowsky et al., 1965; Orekhov et al., 1994,1995). The drawbacks of this method are (i) probehead overheating inherent to CPMG measurements; and (ii) difficulties in suppressing the contribution to relaxation of the antiphase coherences created by scalar coupling, which shortens the measured transverse relaxation rates (Peng et al., 1991a,b). The CPMG delays which can safely be used find their inferior limit in (i) and their superior limit in (ii) (Vold and Vold, 1976). Thus, the accessible range of detectable exchange rates is considerably reduced. The second method is based on measurements of the ^{15}N spin-lattice relaxation in the presence of an on-resonance rf field ($R_{1\rho}$) as a function of its amplitude (Deverell et al., 1970; Brüschweiler and Ernst, 1992; Peng and Wagner, 1992; Szyperski et al., 1993). The drawbacks of this method are (i) again a limited range of rf field strengths due to overheating problems; and (ii) offset dependence of the relax-

*The experiments were performed on the spectrometers of the Laboratoire Commun de RMN, CEA Saclay, France.
**To whom correspondence should be addressed.
Abbreviations: CPMG, Carr–Purcell–Meiboom–Gill; CSA, chemical shift anisotropy; DD, dipole–dipole; HSQC, heteronuclear single quantum correlation; NOE, nuclear Overhauser effect; NOESY, nuclear Overhauser effect spectroscopy; TOCSY, total correlation spectroscopy; TPPI, time-proportional phase increment.

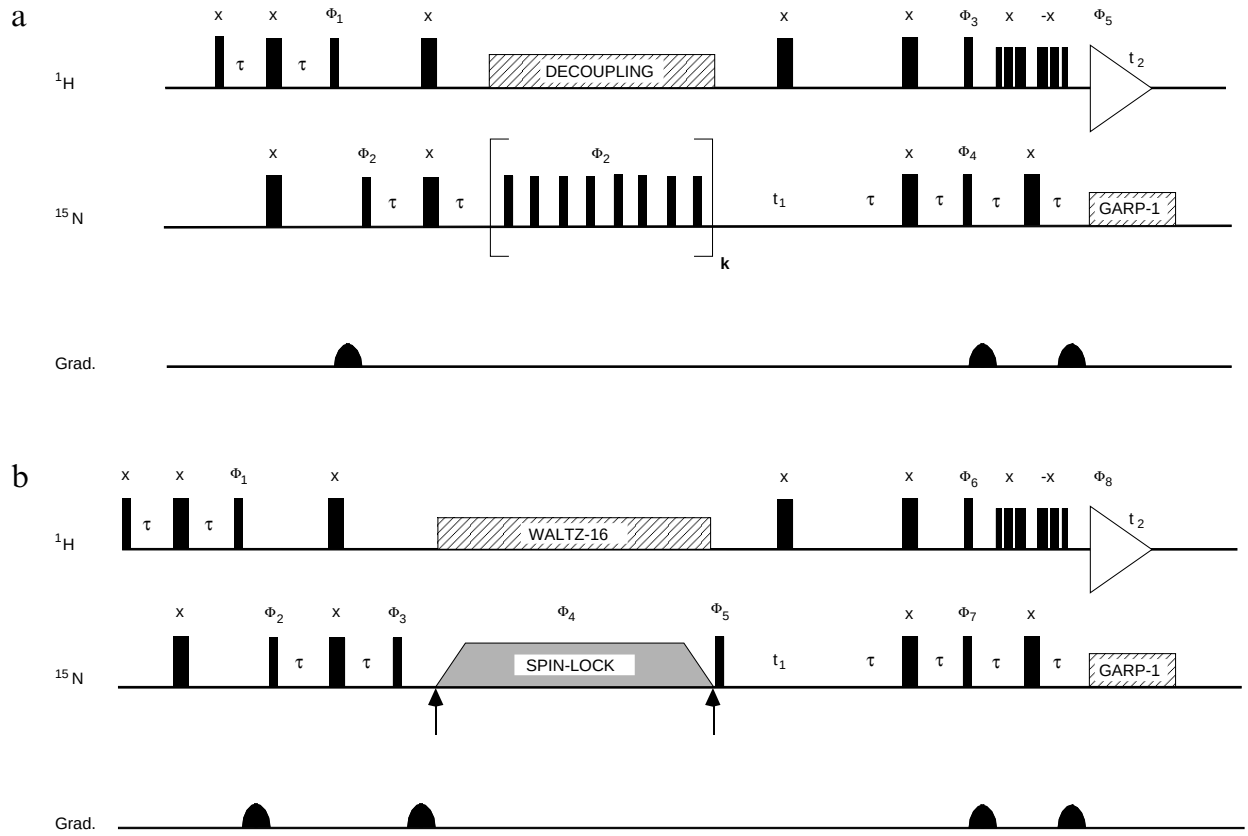

Fig. 1. Pulse schemes used for the measurement of (a) R_2^{CPMG} and (b) $R_{1\rho}(\theta,\omega_1)$. The narrow and wide solid bars represent 90° and 180° hard pulses, respectively. The hard pulses are centered in the ^{1}H and ^{15}N spectra. The value of τ is set to 2.75 ms. Water suppression is achieved with the 3-9-19 WATERGATE sequence. In order to increase sensitivity by minimizing the period during which magnetization is in the transverse plane, the WATERGATE pulse train replaces the last 180° proton pulse. (a) The ^{1}H decoupling during the relaxation delay is either a 180° centered between the fourth and the fifth CPMG ^{15}N 180° pulses, or a WALTZ-4 synchronized on a cycle (CPMG delay – ^{15}N 180° pulse – CPMG delay); a supercycle was added to obtain a WALTZ-16 decoupling scheme. The minimum CPMG cycle is 8 times (CPMG delay – ^{15}N 180° pulse – CPMG delay), i.e, about 8 ms. The mixing time was equal to k times the minimum CPMG cycle. The gradient strengths are 3.5, 12.5 and 12.5 G/cm, respectively. The phase cycling employed is Φ_1 = y,–y; Φ_2 = x,x,–x,–x; Φ_3 = 4(x),4(–x); Φ_4 = 8(x),8(–x); Φ_5 = x,–x,–x,x,–x,x,x,–x,–x,x,x,–x,x,–x,–x,x. After 16 scans, the phase of the first ^{15}N 180° pulse after the evolution period t_1 is inverted without changing the receiver phase. This pulse and the pulse at the center of the evolution period are composite pulses. Quadrature in the F1 dimension is achieved via TPPI on Φ_4. (b) The first arrow corresponds to the change of ^{15}N frequency from on-resonance to off-resonance and the second corresponds to the opposite switch. The gradient strengths are 3.5, 4.5, 12.5 and 12.5 G/cm, respectively. A composite 180° pulse ($90^\circ_x 180^\circ_y 90^\circ_x$) is applied at the center of the t_1 evolution period. The phase cycling 1 is Φ_1 = y,y,–y,–y; Φ_2 = x,–x; Φ_3 = y,–y,–y,y; Φ_4 = 8(x),8(–x),8(y),8(–y); Φ_5 = x,–x; Φ_6 = 4(x),4(–x); Φ_7 = y,y,–y,–y; Φ_8 = x,–x, –x,x,–x,x,x,–x. The phase cycling 2 is Φ_1 = y,y,–y,–y; Φ_2 = x,–x; Φ_3 = 2(y,–y,–y,y),2(–y,y,y,–y); Φ_4 = 8(x),8(–x),8(y),8(–y); Φ_5 = x,–x; Φ_6 = 4(x),4(–x); Φ_7 = y,y,–y,–y; Φ_8 = (x,–x,–x,x),2(–x,x,x,–x),(x,–x,-x,x). Quadrature in the F1 dimension is achieved via States-TPPI on Φ_5.

ation parameter (Peng et al., 1991b). In both methods, the range of detectable exchange rates depends on the relative proportions of the conformational populations and on their difference in resonance frequency. Since it may be possible, by using another static magnetic field strength, to change the contribution due to this difference of resonance frequencies, the last two terms may be determined separately (Barchi et al., 1994; Desvaux et al., 1995b; Peng and Wagner, 1995).

We have recently reported a ^{1}H NMR method designed to explore fast chemical exchange processes with characteristic times in the microsecond to millisecond range (Desvaux et al., 1995b). This method is based on the measurement of relaxation rates along an effective field axis OZ tilted by an angle θ away from the static magnetic field axis Oz. The magnetization vectors are experimentally aligned with OZ by the use of an off-resonance rf irradiation (Jacquinot and Goldman, 1973; James et al., 1977). The angle θ can be varied by choosing the frequency offset Δ and/or the rf field strength ω_1:

$$\theta = \arctan(\omega_1/\Delta) \quad (1)$$

the effective field amplitude Ω in the rotating frame being given by

$$\Omega^2 = \Delta^2 + \omega_1^2 \quad (2)$$

Our approach enables the measurement of ^{1}H dipolar and CSA longitudinal and transverse relaxation rates as well

as the determination of the parameters characterizing the fast chemical exchange processes. The limitations of the on-resonance methods (very fast motions and angular dispersion) are avoided. Indeed, increasing the offset Δ has two main effects: (i) it gives access to large effective field amplitudes Ω and consequently to large values of exchange rates $1/\tau_e$ without any overheating problem; and (ii) it reduces the range of effective angles θ. However, the contribution to relaxation of fast chemical exchange decreases. Recently, Akke and Palmer (1996) have suggested a similar experiment. Their method is based on the sole variation of the angle θ through variation of the offset Δ at constant rf field amplitude ω_1. It results that, at the same time, the transverse contribution to relaxation due to motions in the picosecond–nanosecond time scale and the fast chemical exchange contribution varies. To allow a separation, the authors fix the dipolar and CSA contribution by assuming a model for the motion of the ^{15}NH vector. The only remaining unknown is then the fast chemical exchange contribution whose parameters can be fitted. In fact, this assumption has been shown to be useless since variation of the rf field strength at constant angle θ makes it possible to distinguish the two kinds of contribution (Desvaux et al., 1995b). It seems, consequently, relevant to explore the extension to the heteronuclear case of the method developed for characterizing fast chemical exchange by ^{1}H NMR.

In this article, we report the measurement (on a fully ^{15}N-enriched protein) of heteronuclear off-resonance relaxation rates at different angles θ and different effective field amplitudes Ω, obtained by varying either the frequency offset Δ and/or the rf field strength ω_1. We thus determine the ^{15}N longitudinal and transverse self-relaxation rates. By comparing them to the ones obtained by the usual sequences measuring the longitudinal and transverse self-relaxation rates, assessment of the procedure consisting in using an off-resonance rf field in heteronuclear relaxation studies is achieved. This method also allows us to explore the possible presence of fast chemical exchange processes without using any motion model. A complementary investigation based on the Lipari–Szabo model is presented.

Materials and Methods

NMR experimental conditions

Spectra were acquired at 35 °C on a 5 mM sample of ^{15}N-labelled toxin α at pH 3.5. Toxin α is a 61 amino acid protein which has originally been extracted from the venom of *Naja nigricollis* (Fryklund and Eaker, 1975) and which adopts the 'three-finger' fold (Zinn-Justin et al., 1992); ^{15}N labelling of the sample was carried out as described by Drevet et al. (in press). Assignment of the ^{15}N resonances was performed on the basis of the ^{1}H assignment (Zinn-Justin et al., 1992) by analyzing HSQC (Bodenhausen and Ruben, 1980), HSQC-TOCSY (Otting and Wüthrich, 1988) and HSQC-NOESY experiments (Bax et al., 1990; Norwood et al., 1990). Relaxation measurements were performed at 11.7 T on Bruker AMX and DRX spectrometers equipped with inverse broadband probeheads with either Z or three axes pulsed field gradients. Water suppression was achieved using the WATERGATE sequence (Piotto et al., 1992). The 2D matrices were composed of 1024×256 data points with 32 scans per t_1 value. The spectral widths were 2790 and 2000 Hz in the proton and nitrogen dimensions, respectively. All data sets were Fourier-transformed after application of 90° shifted sine-bell apodization and zero-filling in both dimensions to yield matrices of 1024×1024 points, using the program FELIX 95.0 (MSI/Biosym, San Diego, CA, U.S.A.). Peak heights were measured on each 2D spectrum using FELIX macros written by Mikael Akke.

Reference experiments

Measurement of the ^{15}N longitudinal self-relaxation rate by inversion-recovery ($R_1^{\text{Inv-Rec}}$), of the ^{15}N transverse self-relaxation rate by CPMG (R_2^{CPMG}) and of the ^{1}H$\rightarrow^{15}$N NOE was carried out using the pulse schemes published by Kay et al. (1992). In the case of R_2^{CPMG} measurement, two experiments were performed (Fig. 1a). In the first one, ^{1}H decoupling was obtained by the application of π pulses on the ^{1}H channel (Boyd et al., 1990; Kay et al., 1992; Palmer et al., 1992). In the second one, it was achieved through a synchronized WALTZ-16 sequence centered on the amide frequency domain (Shaka et al., 1983; Shaka and Keeler, 1987; Palmer et al., 1992). The equivalence of the two decoupling schemes relative to cross relaxation arising from interference effects between CSA and dipolar interaction was firstly checked in longitudinal relaxation measurements (the average relative standard deviation calculated between the two data sets was 4%) and then in transverse relaxation measurements (an equivalent calculation yielded 5%). In the following, the used R_2^{CPMG} values are the average values of the two measures. The $R_1^{\text{Inv-Rec}}$ experiments were recorded with relaxation delays of 20, 50, 100, 200, 500, 1000 and 1500 ms. The R_2^{CPMG} experiments were carried out with relaxation delays of 9, 18, 28, 46, 74, 92, 184, 368, 552 and 768 ms. The heteronuclear ^{1}H$\rightarrow^{15}$N NOE values were obtained on the basis of spectra recorded with proton presaturation during 4 s and spectra recorded without presaturation. Quadrature detection in the indirect dimension used the TPPI scheme for the R_2^{CPMG} experiments and the States-TPPI phase scheme for the $R_1^{\text{Inv-Rec}}$ and heteronuclear ^{1}H$\rightarrow^{15}$N NOE experiments (Marion et al., 1989).

Off-resonance self-relaxation measurements

The $R_{1\rho}(\theta,\omega_1)$ experiments were performed with the pulse sequence displayed in Fig. 1b. This sequence directly derives from the ^{15}N longitudinal self-relaxation rate

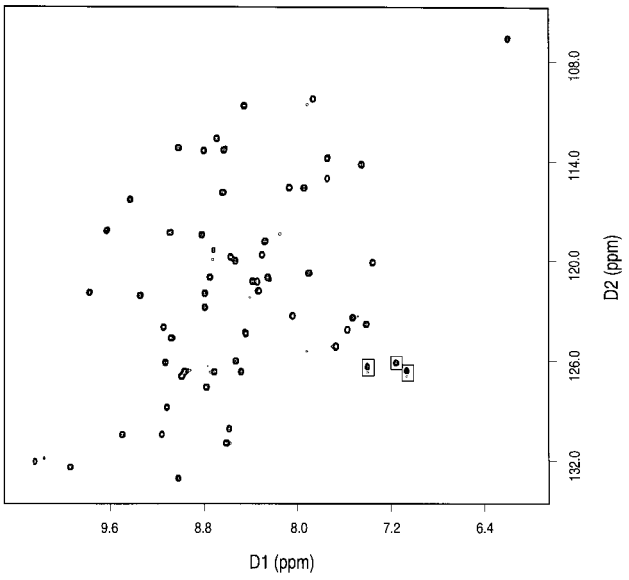

Fig. 2. Contour plot of a ^{15}N-^{1}H experiment recorded with the off-resonance $R_{1\rho}(\theta,\omega_1)$ sequence on a ^{15}N-enriched sample of toxin α. For this particular spectrum, the angle θ was 5°, the rf field strength ω_1 was 1.9 kHz and the mixing time was 30 ms. The experiment time was about 4 h. One can notice the good dispersion of the ^{15}N-^{1}H correlations. The three boxed peaks are folded-back in the indirect dimension F1 and correspond to arginine side-chain ($N^{\varepsilon}H^{\varepsilon}$) correlations.

measurement sequence. The major modification consists in applying an rf spin-lock of strength ω_1 at an offset Δ from the center of the nitrogen spectrum during the mixing time. The magnetization is then locked along an axis OZ making an angle θ with the static field direction. Progressive increase of the rf amplitude at the beginning of the spin-lock (and progressive decrease at its end) ensures adiabatic rotation of the magnetization from the Oz axis to the effective field axis OZ (and back to Oz at the end of the mixing time) (Desvaux et al., 1995a). This is obtained by using a trapeze-shaped pulse composed of 2048 complex points. The typical value of the adiabatic rotation duration is about 3 ms. As magnetization is aligned with Oz, the use of adiabatic rotations suppresses the requirement of adjusting the phase shift between on-resonance and off-resonance rf pulses when only hard pulses are used (Akke and Palmer, 1996). A typical spectrum acquired by this sequence on toxin α is shown in Fig. 2.

In order to assess the relevance of studying a variation of the ^{15}N self-relaxation rates as a function of the angle θ and the effective field amplitude Ω, we have determined the ^{15}N B_1 field inhomogeneity *in amplitude* principally inherent to the coil design on our probehead. The B_1 field inhomogeneity, defined as the ratio of the width at $P_{max}/2$ over the amplitude B_1 at P_{max}, where P_{max} is the maximum of probability, is found to be equal to 5%. The distribution of angle θ due to B_1 inhomogeneity is then negligible relatively to other errors. The distribution of B_1 amplitude is provided as supplementary material.

As suggested in the case of proton, we have considered the sequence with irradiation at one offset (either upfield or downfield) or at two offsets (successive scans recorded with opposite offset shift). This last solution has been shown to decrease the effective angular dispersion but no exact analytical solution can be calculated for long mixing times (Schleucher et al., 1995; Desvaux and Goldman, 1996). It results (in the heteronuclear case) in a simpler treatment for determination of the longitudinal and transverse self-relaxation rates, and also in a loss of precision when the study deals with characterization of the exchange processes since the effective angle cannot further be exactly determined for each ^{15}N nucleus.

Two phase cyclings were also considered. For the two-offset $R_{1\rho}(\theta,\omega_1)$ experiment, the classical phase cycling (cycle 1) for ^{15}N heteronuclear longitudinal self-relaxation measurement has been used. Under such conditions, magnetization relaxes towards its steady-state value which depends on θ and Ω (Desvaux et al., 1995b). This sequence consequently requires long irradiation times for a precise determination of the three parameters which have to be fitted: initial magnetization, relaxation rate and steady-state magnetization. In order to limit probehead overheating when long irradiations are applied, we have used a modified phase cycling (cycle 2) for the 'one-offset' $R_{1\rho}(\theta, \omega_1)$ experiment. This phase cycling is twice longer than the precedent, but magnetization then relaxes towards 0. It has experimentally been checked (data not shown) that the signal effectively vanishes at long mixing times. Although short irradiations are used, the precision on the determined self-relaxation rate values is still good since only two parameters (initial intensity and self-relaxation rate) have to be fitted (Sklenář et al., 1987). Seven mixing times were used in the $R_{1\rho}(\theta,\omega_1)$ experiments: 30, 60, 150, 300, 500, 800 and 1200 ms for cycle 1 and 30, 50, 70, 100, 150, 300 and 500 ms for cycle 2. Some experiments among all the acquired ones, however, exhibit strong baseline distortions (in a reduced frequency domain) arising from the residual water signal. When a cross peak is affected, the precision of the self-relaxation rate determination decreases and we have consequently disregarded the complete curve. This explains the non-constant number of points of Fig. 5.

In the sequence of Fig. 1b, relaxation induced by cross-correlation between DD and CSA interaction (Boyd et al., 1990) is suppressed by using the same WALTZ-16 decoupling scheme as in longitudinal $R_1^{\text{Inv-Rec}}$ and transverse R_2^{CPMG} relaxation experiments. From a theoretical point of view, in the laboratory frame, as soon as the proton spins are spin-locked in the transverse plane, the two coherences N_Z and $2N_ZH_Z$ do not precess at the same frequency (Z being the effective field axis in the ^{1}H and ^{15}N rotating frames). Thus, cross relaxation through cross-correlation is no longer secular (Goldman, 1993), and the CSA/DD cross-correlation rate $N_Z \rightarrow 2N_ZH_Z$ vanishes.

Fitting procedure

Evolution of the magnetization in the $R_1^{Inv\text{-}Rec}$ and R_2^{CPMG} experiments was fitted by three- and two-parameter exponentials, respectively. For the $R_1^{Inv\text{-}Rec}$, R_2^{CPMG} and $^1H\rightarrow{}^{15}N$ NOE data, the errors were taken as the root-mean-square deviation of two separate sets of measure and were found to be in agreement with the error computed by Monte Carlo simulation. The one- and two-offset $R_{1\rho}(\theta,\omega_1)$ experimental decays were fitted to a two- and three-parameter exponential, respectively. Errors on the $R_{1\rho}(\theta,\omega_1)$ relaxation rates were computed by Monte Carlo simulation.

The self-relaxation rate $R_{1\rho}(\theta,\omega_1)$ of the ^{15}N magnetization aligned with the effective field axis OZ can easily be deduced from the proton case (Davis et al., 1994; Desvaux et al., 1995b):

$$R_{1\rho}(\theta,\omega_1) = \cos^2\theta\, R_1 + \sin^2\theta\, R_2 + R_{ex}(\theta,\omega_1) \qquad (3)$$

where R_1 and R_2 are the longitudinal and transverse self-relaxation rates for the fast motions contribution (correlation time inferior to 1 μs, prevailing mechanisms: DD and CSA interactions) and $R_{ex}(\theta,\omega_1)$ is the relaxation rate associated with the slow motion processes (chemical exchange contribution). Assuming a two-site model with populations p_a and p_b, a resonance frequency difference $\delta\nu$ between the two conformations and an exchange rate $1/\tau_e$, $R_{ex}(\theta,\omega_1)$ can be expressed as (Davis et al., 1994; Desvaux et al., 1995b; Akke and Palmer, 1996)

$$R_{ex}(\theta,\omega_1) = 4\pi^2\, p_a p_b \sin^2\theta\, \delta\nu^2\, \tau_e/(1+\Omega^2\tau_e^2) \qquad (4)$$

Since only one static magnetic field has been employed for the measurements, the two parameters $p_a p_b$ and $\delta\nu$ cannot be separated. We have chosen to consider in the following two equally populated families. This induces an underestimation of the derived resonance frequency difference values.

The two-offset $R_{1\rho}(\theta,\omega_1)$ values were used to determine the longitudinal R_1 and transverse R_2 self-relaxation rates and to identify the ^{15}NH vectors exhibiting fast chemical exchange processes. This procedure was based on a least-squares fitting of Eq. 3 using the Marquard algorithm (Press et al., 1992). Errors on R_1 and R_2 were computed by Monte Carlo simulation. Thus, normalized χ^2 values were determined and statistical tests on the fit quality could be carried out. Comparisons of the fit quality with and without taking into account the experimental values $R_1^{Inv\text{-}Rec}$ and R_2^{CPMG} or with and without assuming a chemical exchange contribution $R_{ex}(\theta,\omega_1)$ were performed using the determined χ^2 values through an F-test. The results of this F-test are given through the probability P that the fit improvement is not due to chance (Mack, 1967; Press et al., 1992).

The one-offset $R_{1\rho}(\theta,\omega_1)$ values were used to determine the exchange correlation time τ_e and the chemical shift difference $\delta\nu$. In this procedure, the numerical treatment consisted of the computation for each $R_{1\rho}(\theta,\omega_1)$ of a rate $R_{1\rho}(90°,\omega_1/\sin\theta)$, using Eqs. 3 and 4 and the value R_1 of the longitudinal relaxation rate previously determined (Akke and Palmer, 1996):

$$\begin{aligned} R_{1\rho}(90°,\omega_1/\sin\theta) - R_1 &= (R_{1\rho}(\theta,\omega_1) - R_1)/\sin^2\theta \\ &= (R_2 - R_1) + R_{ex}/\sin^2\theta \end{aligned} \qquad (5)$$

Then, the variations of $R_{1\rho}(90°,\omega_1/\sin\theta) - R_1$ as a function of θ and ω_1 were used to determine τ_e and $\delta\nu$. The data were completed with the R_2^{CPMG} values, which also depend on τ_e and $\delta\nu$. Indeed, for this experiment, as the duration τ_π of the π pulse (143 μs) was not negligible relative to the free evolution time τ (1 ms), we used the average trajectory theory (Griesinger and Ernst, 1988) to estimate the apparent effective field ω_{app}:

$$R_{1\rho}(90°,\omega_{app})(\tau+\tau_\pi) = \tau_\pi\, R_{1\rho}(90°,1/2\tau_\pi) + \tau\, R_{1\rho}(90°,0) \qquad (6)$$

This treatment is justified by the fact that the magnetization decay is slow relative to R_2^{CPMG}. As the apparent field ω_{app} depends on the exchange correlation time, both parameters have iteratively been refined. We have checked that the value of ω_{app} has a small influence on the derived exchange correlation time value.

The transverse relaxation rate R_2 was not directly used in the fit; instead the $R_2 - R_1$ value was randomly varied in a range defined by the values of the surrounding residues (Palmer et al., 1991; Tjandra et al., 1996). Typically 20% of variation was admitted, and the value corresponding to the lowest χ^2 was kept.

Modelfree analysis

The Modelfree 3.1 program based on the Lipari–Szabo model (Palmer et al., 1991) was used to extract for each ^{15}NH vector an exchange term R_{ex}^{LS} from $R_1^{Inv\text{-}Rec}$, an average $\langle R_{1\rho}(90°,\omega_1/\sin\theta)\rangle$ computed from the two-offset set of measured $R_{1\rho}(\theta,\omega_1)$, and $^1H\rightarrow{}^{15}N$ NOE data. Therefore, we assumed an isotropic motion model for toxin α where the global and internal motions are not correlated; the angular part of the spectral density $J(\omega)$ is (Lipari and Szabo, 1982)

$$J(\omega) = 2/5\, [S^2\tau_c/(1+\omega^2\tau_c^2) + (1-S^2)\tau_i/(1+\omega^2\tau_i^2)] \qquad (7)$$

τ_c being the overall isotropic correlation time, τ_m the internal correlation time with $\tau_i = (1/\tau_c + 1/\tau_m)^{-1}$ and S^2 the generalized order parameter. Errors on the average $\langle R_{1\rho}(90°,\omega_1/\sin\theta)\rangle$ values were taken as standard errors calculated on the basis of the two-offset $R_{1\rho}(90°,\omega_1/\sin\theta)$ values. Errors made on R_{ex}^{LS} were calculated on the basis of the errors estimated on $R_1^{Inv\text{-}Rec}$, the 'two-offset' average

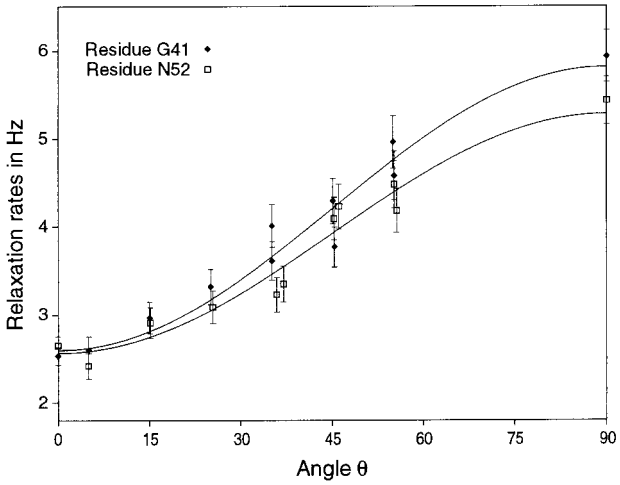

Fig. 3. Experimental ^{15}N self-relaxation rates as a function of the angle θ for the residues Gly^{41} and Asn^{52}. The best-fit theoretical curve using Eq. 3 and assuming no chemical exchange is superimposed. For this fitting procedure, the nine two-offset off-resonance self-relaxation rates $R_{1\rho}(\theta,\omega_1)$, the longitudinal one $R_1^{Inv\text{-}Rec}$ and the transverse one R_2^{CPMG} have been used. The reduced χ^2 values are 1.02 and 0.92, respectively. The presence of several points at the same θ value is due to the use of different effective field amplitudes Ω.

$<R_{1\rho}(90°,\omega_1/\sin\theta)>$ and $^1H\rightarrow{}^{15}N$ NOE rates, and 500 Monte Carlo simulations.

Results and Discussion

Off-resonance self-relaxation measurements

We have measured the two-offset off-resonance ^{15}N self-relaxation rates for nine pairs of (ω_1,θ) values: three rf field strengths (between 1.2 and 2.2 kHz) and six angles θ between 5° and 55°. Assuming that no chemical exchange is present, we have fitted the nine rates obtained with the off-resonance irradiation sequence and the longitudinal $R_1^{Inv\text{-}Rec}$ and transverse R_2^{CPMG} relaxation rates obtained with the classical sequences on the basis of Eq. 3. Figure 3 shows two examples of the corresponding least-squares fitting curves. A good agreement is observed between the expected and observed behavior of $R_{1\rho}(\theta,\omega_1)$ as a function of the angle θ.

To assess the procedure using off-resonance rf irradiation for ^{15}N self-relaxation rate measurements, these fits have been compared to other fits obtained without taking into account the reference longitudinal $R_1^{Inv\text{-}Rec}$ or transverse R_2^{CPMG} self-relaxation rates. Out of the 52 experimental curves, 51 exhibit no significant improvement ($P < 97.5\%$) after removal of the longitudinal self-relaxation rate $R_1^{Inv\text{-}Rec}$. The only discrepancy concerns the nitrogen of residue Tyr^{24} ($P = 97.8\%$). When the transverse self-relaxation rate R_2^{CPMG} is disregarded, at the same level of confidence, 41 cases out of the 52 do not present significant improvement in the fitting procedure. The 11 nitrogen nuclei which exhibit a discrepancy between their fitted transverse self-relaxation rate R_2 and the one measured by a CPMG sequence R_2^{CPMG} belong to residues Cys^3, Cys^{17}, Glu^{20}, Thr^{21}, Lys^{26}, Ile^{35}, Thr^{44}, Gly^{48}, Lys^{50}, Leu^{51} and Lys^{58} (Table 1, Fig. 4). In all cases, the fitted transverse self-relaxation rate R_2 is smaller than the measured one R_2^{CPMG}. This result is in agreement with the theory as soon as fast chemical exchange is present (Eq. 3). Thus, we consider that the statistical tests validate the experimental procedure using off-resonance rf irradiation

TABLE 1
^{15}N TRANSVERSE SELF-RELAXATION RATES AND EXCHANGE CORRELATION TIMES OF THE RESIDUES EXHIBITING CHEMICAL EXCHANGE

Residue	R_2^{CPMG} (Hz)	R_2 [a] (Hz)	$<R_{1\rho}(90,\omega_1/\sin\theta)>$ [b] (Hz)	R_{ex}^{LS} [c] (Hz)	Discrepancy R_2^{CPMG},R_2 [d]	Variation with Ω [e]	τ_e [f]
Cys^3	8.31	6.74	6.68	1.55	99.1	+	120 μs
Asn^5	7.16	6.50	6.69	1.12			< 50 μs
Ser^9	6.54	6.09	6.25	1.55			< 50 μs
Cys^{17}	13.02	10.12	10.06	5.27	99.6	+	20–200 μs
Glu^{20}	7.90	6.28	6.38	1.77	98.6	+	135 μs
Thr^{21}	11.40	9.23	9.22	4.46	97.7	+	75 μs
Lys^{26}	7.91	4.99	5.00	–	99.8	+	240 μs
Ile^{35}	7.36	5.29	5.22	0.25	99.8	+	150 μs
Thr^{44}	6.86	4.81	4.75	–	99.2		> 1 ms
Gly^{48}	7.77	5.25	5.21	0.75	99.9		> 1 ms
Lys^{50}	10.30	5.83	5.84	0.78	99.9		> 1 ms
Leu^{51}	6.50	4.95	4.95	–	98.4	+	290 μs
Lys^{58}	6.05	5.22	5.29	–	98.3		> 1 ms

[a] The R_2 values correspond to those obtained without using R_2^{CPMG} in the fitting procedure.
[b] $<R_{1\rho}(90,\omega_1/\sin\theta)>$ is the value used in the Modelfree software; [c] R_{ex}^{LS} is the exchange contribution obtained by this computation.
[d] Residues exhibiting a significant improvement in the fit when R_2^{CPMG} is not considered. The value is the probability P (in %) of the F-test that the discrepancy between R_2 and R_2^{CPMG} is not due to chance (see text). For Asn^5 and Ser^9, P is 84% and 67%, respectively.
[e] Residues for which, in the one-offset experiment, a variation of $R_{1\rho}(90,\omega_1/\sin\theta)$ as a function of Ω is observed.
[f] Range of exchange correlation time τ_e determined by combining all measurements.

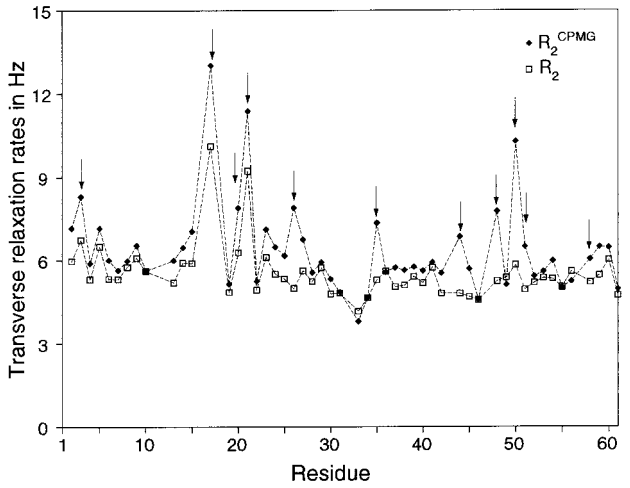

Fig. 4. Comparison of the transverse self-relaxation rates R_2^{CPMG} obtained by the CPMG experiment (Fig. 1a) and the fitted ones R_2 as a function of the corresponding residue number. The values of R_2 were obtained by a fit with Eq. 3 without chemical exchange. The set of self-relaxation rates was constituted by the longitudinal one $R_1^{Inv\text{-}Rec}$ and the two-offset off-resonance ones $R_{1\rho}(\theta,\omega_1)$. The average relative standard deviation between the two data sets is 5%. The arrows indicate the residues where the statistical tests (see text) have revealed a significant difference between R_2 and R_2^{CPMG}.

for the determination of the ^{15}N longitudinal R_1 and transverse R_2 self-relaxation rates arising from motions with correlation times in the nanosecond time range.

Using the same set of relaxation rates constituted by the nine $R_{1\rho}(\theta,\omega_1)$, and the measured $R_1^{Inv\text{-}Rec}$ and R_2^{CPMG}, we have considered the possible improvement of the fits if a chemical exchange contribution was added to the expression of $R_{1\rho}(\theta,\omega_1)$. The four unknowns of Eqs. 3 and 4 have then been fitted. Only the 11 previously identified nitrogens present a significant improvement ($P > 92\%$) of their fit when the more complex fitting curve is used to describe the experimental relaxation rates. We conclude that the relaxation dynamics of these 11 nitrogen nuclei should contain a contribution due to motions with correlation times superior to 1 μs.

Measurement of the off-resonance ^{15}N self-relaxation rates for nine pairs of (ω_1,θ) values has allowed us to validate the heteronuclear off-resonance sequence, by showing that the $R_1^{Inv\text{-}Rec}$ values and most of the R_2^{CPMG} values can be deduced from the $R_{1\rho}(\theta, \omega_1)$ data. It has also enabled the identification of 11 nitrogens having significantly different R_2^{CPMG} and R_2 values, in agreement with the presence of fast chemical exchange contributing to their relaxation rates (Table 1, Fig. 4). However, at this step the correlation time τ_e and the chemical shift difference $\delta\nu$ of these exchange processes cannot be determined with a high confidence.

Determination of exchange rates

We have explored the possibility of determining exchange correlation time for the 11 nitrogens of toxin α which exhibit a significant discrepancy between the measured R_2^{CPMG} and the fitted one R_2. This requires an increase of precision in the determination of the self-relaxation rate $R_{1\rho}(\theta,\omega_1)$. The advantage of the two-offset sequence (suppression of the problems due to angular dispersion) seems then poor compared to the loss of precision inherent to this experiment. The one-offset sequence is undoubtedly more adapted to the precise characterization of the exchange parameters τ_e and $\delta\nu$. We have measured nine other off-resonance relaxation rates using only the 'one-offset' irradiation (either upfield or downfield). For these nine experiments, the average angle θ was 55° and the values of the rf field strength ω_1 ranged from 1200 to 1800 Hz. The mean effective field amplitude Ω varied from 1500 to 2200 Hz. However, as one-offset irradiation was used, this range increased for residues on the edges of the nitrogen spectrum. Since the distribution of the explored angles θ was limited, we disregard the direct fitting procedure of Eq. 3. A rate $R_{1\rho}(90°,\omega_1/\sin\theta)$ was computed on the basis of each $R_{1\rho}(\theta,\omega_1)$ value, and analysis of the variations of $R_{1\rho}(90°,\omega_1/\sin\theta)$ as a function of Ω allowed us to characterize τ_e and $\delta\nu$.

On the basis of this analysis, the 11 nitrogens could be separated into three classes (Table 1). The first class contains residues Thr^{44}, Gly^{48}, Lys^{50} and Lys^{58}. The nitrogens of these residues exhibit average $R_{1\rho}(90°,\omega_1/\sin\theta)$ of the same order as the neighboring residue R_2 values (Fig. 4) and no significant variation of $R_{1\rho}(90°,\omega_1/\sin\theta)$ in the range of effective field amplitudes explored. It results that τ_e should be longer than about 1 ms. The second class corresponds to residues Lys^{26}, Ile^{35} and Leu^{51} for which the average $R_{1\rho}(90°,\omega_1/\sin\theta)$ is not very different from the surrounding residue R_2 values (Fig. 4), but a variation as

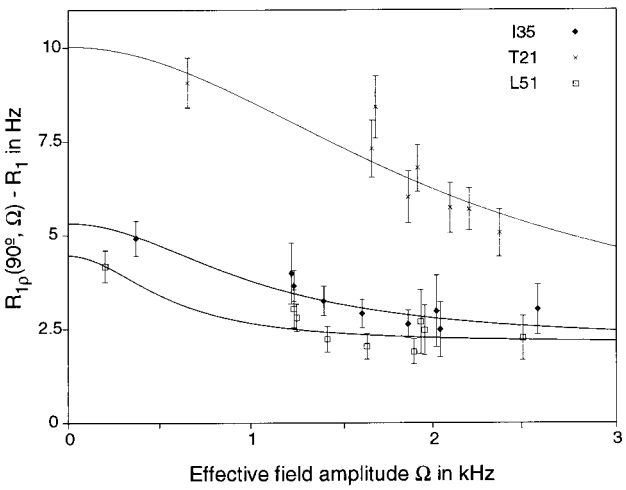

Fig. 5. ^{15}N self-relaxation rate $R_{1\rho}(90°,\omega_1/\sin\theta) - R_1$ for residues Thr^{21}, Ile^{35} and Leu^{51} as a function of the effective field amplitude $\Omega = \omega_1/\sin\theta$. The best-fit theoretical curve using Eqs. 4 and 5 is superimposed. The best-fit correlation times for Thr^{21}, Ile^{35} and Leu^{51} are 75, 150 and 290 μs and the reduced normalized χ^2 values are 0.94, 0.28 and 0.68, respectively.

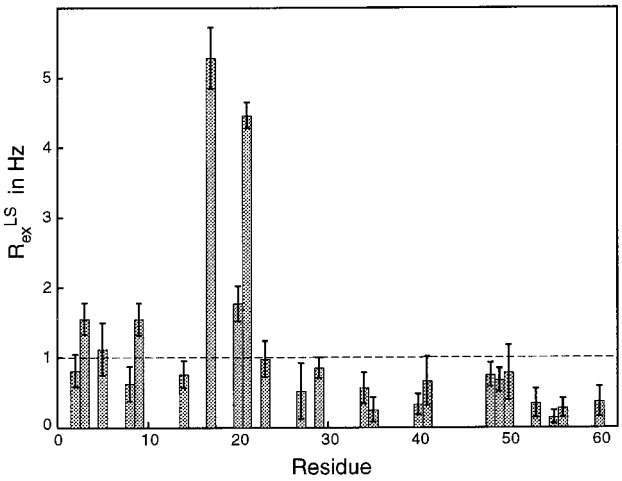

Fig. 6. Values of the chemical exchange contribution R_{ex}^{LS} in Hz obtained after the assumption of a Lipari–Szabo motion model as a function of the corresponding residue number. These values were calculated on the basis of the longitudinal $R_1^{Inv\text{-}Rec}$ self-relaxation rate, the two-offset average transverse self-relaxation rate $<R_{1\rho}(90°,\omega_1/\sin\theta)>$ and NOE values using the Modelfree 3.1 software of Palmer et al. (1991). The error bars have been deduced from 500 Monte Carlo simulations.

a function of ω_1 is observed (Fig. 5). The fitted exchange correlation time is in the range 100–400 μs. Finally, the last class corresponds to residues Cys^3, Cys^{17}, Glu^{20} and Thr^{21} for which the average $R_{1\rho}(90°,\omega_1/\sin\theta)$ is larger than the R_2 values of the surrounding amino acids (Fig. 4). By Monte Carlo numerical simulations, we conclude that these experimental results are compatible with motions on a time scale of about 20–200 μs. For residues Cys^3, Glu^{20} and Thr^{21}, the dependence of $R_{1\rho}(90°,\omega_1/\sin\theta)$ on Ω was sufficiently good (see Fig. 5) to allow a confident determination of τ_e (~120, ~135 and ~70 μs, respectively) and δν (~1, ~1 and ~2 ppm, respectively) for an equally distributed two-site model.

It seems relevant to discuss the range of exchange correlation times we have access to. For slow motions ($\tau_e > 1$ ms), the limitation relies on the obtaining of small Ω values. This requires low rf field amplitude and small offset values (Eq. 2). These two requirements are experimentally difficult to achieve in an off-resonance measurement: firstly, experimental calibration of a low-power rf irradiation on an inverse probehead is not precise; secondly, rf irradiation near resonance conditions may induce Hartmann–Hahn coherence transfer with proton; and, thirdly, our underlying assumptions require Ω large relative to $^1J_{NH}$ scalar coupling values. On the other hand, for short exchange correlation time determination ($\tau_e < 50$ μs), large values of Ω are required. The hardware restrains the rf field amplitude to about 2.3 kHz on our spectrometer. Obviously, by choosing a large offset, large effective field amplitudes Ω are obtained, but the resulting small θ values induce a large error on the computed $R_{1\rho}(90°,\omega_1/\sin\theta)$. To avoid this trouble, a solution may be to determine a large number of $R_{1\rho}(\theta,\omega_1)$ values with a high precision, and finally fit the experimental data directly using Eq. 3. Our one-offset measurements were not sufficiently numerous to achieve such a task, and the variation of $R_{1\rho}(90°,\omega_1/\sin\theta)$ with Ω could be confidently fitted for only six residues.

Exploration of chemical exchange using the Lipari–Szabo motion model

We investigated the contribution to transverse relaxation of fast chemical exchange processes in toxin α by applying the Lipari and Szabo analysis (1982) to a set of values comprising the $R_1^{Inv\text{-}Rec}$, the two-offset average value $<R_{1\rho}(90°,\omega_1/\sin\theta)>$ and the $^1H\rightarrow{}^{15}N$ NOE data. In the two-offset $<R_{1\rho}(90°,\omega_1/\sin\theta)>$ measurement, the smallest value of the effective field amplitude Ω is about 2 kHz, so that all chemical exchange contributions, with correlation times longer than about 0.5 ms, vanish. Using this set of data, we deduced that six nitrogens show an R_{ex}^{LS} value greater than 1 Hz, that is twice the maximal error calculated for R_{ex}^{LS} (Table 1, Fig. 6). These six nitrogens are (i) residues Cys^3, Cys^{17}, Glu^{20} and Thr^{21} which have already been identified as corresponding to motions on a time scale of about 20–200 μs; and (ii) residues Asn^5 and Ser^9 which do not present any significant discrepancy between the measured R_2^{CPMG} and the fitted one R_2 . The time scale of the Asn^5 and Ser^9 exchange process is then in the 1–50 μs range, since no significant transverse relaxation rate variation between 0 and 3.3 kHz was observed. Finally, Fig. 6 shows that an R_{ex}^{LS} value smaller than 1 Hz is detected for each residue exhibiting a chemical exchange contribution whose correlation time is longer than about 200 μs in the one-offset experiment (Lys^{26}, Ile^{35}, Thr^{44}, Gly^{48}, Lys^{50}, Leu^{51} and Lys^{58}).

The complete agreement between the one-offset experiment and the Modelfree analyses shows that, for toxin α, application of the Lipari–Szabo model is probably appropriate. This is substantiated by hydrodynamic computations (Garcia de la Torre and Bloomfield, 1981) which reveal that the principal moments of the inertia tensor have ratios 1:0.85:0.8. A similar result has already been found by Wagner and co-workers on eglin c (Peng and Wagner, 1995; Lefèvre et al., 1996). These authors stressed that, for their protein, the spectral density mapping and Modelfree analyses led to similar conclusions. However, this is not a general case; various proteins have already been shown to exhibit a more complex dynamics with, in particular, no unique global correlation time or no isotropic behavior (Brüschweiler et al., 1995; Farrow et al., 1995; Tjandra et al., 1995a,b,1996).

Conclusions

Measurement of the two-offset off-resonance ^{15}N self-relaxation rates for nine pairs of (θ,ω_1) values has allowed

the validation of the heteronuclear off-resonance sequence, by showing that the $R_1^{Inv\text{-}Rec}$ values and most of the R_2^{CPMG} values can be deduced from the $R_{1\rho}(\theta,\omega_1)$ data. The proposed two-offset off-resonance $R_{1\rho}(\theta,\omega_1)$ sequence is an answer to the two main drawbacks of on-resonance $R_{1\rho}$ measurements: (i) it gives access to large effective field amplitudes and consequently to large values of exchange rates without any overheating trouble; and (ii) it reduces the range of effective θ angles. It thus allows the measurement of transverse relaxation rates with the lowest possible exchange contribution, the data processing being facilitated by the absence of offset corrections. The $R_{1\rho}(\theta, \omega_1)$ data can be exploited in different ways. Firstly, it can simply be compared to R_2^{CPMG} data. By this method, 11 nitrogens of toxin α have been shown to exhibit a significant fast chemical exchange contribution to their relaxation rates. Secondly, the $R_{1\rho}(\theta,\omega_1)$ data can be used in a spectral density mapping or Modelfree analysis, in order to characterize the exchange processes in the range 1–500 μs.

Measurement of the one-offset off-resonance ^{15}N self-relaxation rates for nine pairs of (θ,ω_1) values has allowed us to increase the accuracy of the self-relaxation rate $R_{1\rho}(\theta,\omega_1)$ determination. On the basis of these experiments, the exchange parameters τ_e and $\delta\nu$ of the 11 previously identified nitrogens of toxin α were evaluated. Thus, Thr^{44}, Gly^{48}, Lys^{50} and Lys^{58} nitrogens exhibit motions on a time scale of 1–100 ms, the slow motion characteristic time scale of Lys^{26}, Ile^{35} and Leu^{51} is on the order of 200 μs while Cys^3, Cys^{17}, Gly^{20} and Thr^{21} are subjected to motions on a time scale of 100 μs. For six of them, significant and coherent variations of $R_{1\rho}(90°,\omega_1/\sin\theta)$ as a function of Ω were observed allowing a better characterization (Fig. 5).

Different chemical or conformational exchange processes on the microsecond–millisecond time scale have been described in proteins (Wagner, 1983; Bai et al., 1993; Szyperski et al., 1993; Lefèvre et al., 1996). A preliminary interpretation of our results can be suggested on the basis of these processes. Firstly, exchange contributions to the Lys^{26}, Ile^{35} and Lys^{50} ^{15}N relaxation rates, which have time scales in the millisecond range, may reflect the ring flip of the two aromatic rings of toxin α, i.e. that of Tyr^{24} and Trp^{28}. Secondly, exchange contributions to the Thr^{44}, Gly^{48} and Leu^{51} ^{15}N relaxation rates, which also have time scales in the millisecond range, may reflect the exchange of the corresponding amide protons with water. Finally, exchange contributions to the Cys^3, Asn^5, Cys^{17}, Glu^{20} and Thr^{21} ^{15}N relaxation rates, which have time scales of about 100 μs, may reflect motions of the (Cys^3,Cys^{23}) and (Cys^{17}, Cys^{40}) disulfide bridges. Based on the three-dimensional structure of toxin α (Zinn-Justin et al., 1992), a more detailed analysis of these slow motions and also of the internal fast motions will be presented in a forthcoming article.

Acknowledgements

The authors greatly acknowledge Dr. M. Akke for providing the FELIX macros used to integrate the signal and Dr. A.G. Palmer III for the Modelfree 3.1 software. M.G. acknowledges IFSBM (Villejuif, France) for a fellowship.

References

Akke, M. and Palmer III, A.G. (1996) *J. Am. Chem. Soc.*, **118**, 911–912.

Bai, Y., Milne, J.S., Mayne, L. and Englander, S.W. (1993) *Proteins Struct. Funct. Genet.*, **17**, 75–86.

Barchi, J.J., Grasberger, B., Gronenborn, A.M. and Clore, G.M. (1994) *Protein Sci.*, **3**, 15–21.

Bax, A., Ikura, M., Kay, L.E., Torchia, D.A. and Tschudin, R. (1990) *J. Magn. Reson.*, **86**, 304–318.

Bodenhausen, G. and Ruben, D. (1980) *Chem. Phys. Lett.*, **69**, 185–188.

Boyd, J., Hommel, U. and Campbell, I.D. (1990) *Chem. Phys. Lett.*, **175**, 477–482.

Brüschweiler, R. and Ernst, R.R. (1992) *J. Chem. Phys.*, **96**, 1758–1766.

Brüschweiler, R., Liao, X. and Wright, P.E. (1995) *Science*, **268**, 886–889.

Carr, H.Y. and Purcell, E.M. (1954) *Phys. Rev.*, **94**, 630–638.

Davis, D.G., Perlman, M.E. and London, R.E. (1994) *J. Magn. Reson.*, **B104**, 266–275.

Desvaux, H., Berthault, P., Birlirakis, N., Goldman, M. and Piotto, M. (1995a) *J. Magn. Reson.*, **A113**, 47–52.

Desvaux, H., Birlirakis, N., Wary, C. and Berthault, P. (1995b) *Mol. Phys.*, **86**, 1059–1073.

Desvaux, H. and Goldman, M. (1996) *J. Magn. Reson.*, **B110**, 198–201.

Deverell, C., Morgan, R.E. and Strange, J.H. (1970) *Mol. Phys.*, **18**, 553–559.

Drevet, P., Lemaire, C., Gasparini, S., Zinn-Justin, S., Lajeunesse, E., Ducancel, F., Trémeau, O., Courson, M., Boulain, J.-C. and Ménez, A. (1997) *Protein Expression Purif.*, **10**, 293–300.

Farrow, N.A., Zhang, O., Forman-Kay, J.D. and Kay, L.E. (1995) *Biochemistry*, **34**, 868–878.

Fryklund, L. and Eaker, D. (1975) *Biochemistry*, **14**, 2865–2871.

Garcia de la Torre, J. and Bloomfield, V.A. (1981) *Q. Rev. Biophys.*, **14**, 81–139.

Goldman, M. (1993) In *Nuclear Magnetic Double Resonance* (Ed., Maraviglia, B.), North-Holland, Amsterdam, The Netherlands, pp. 1–68.

Griesinger, C. and Ernst, R.R. (1988) *Chem. Phys. Lett.*, **152**, 239–247.

Gutowsky, H.S., Vold, R.L. and Wells, E.J. (1965) *J. Chem. Phys.*, **43**, 4107–4125.

Jacquinot, J.F. and Goldman, M. (1973) *Phys. Rev.*, **B8**, 1944–1957.

James, T.L., Matson, G.B., Kuntz, I.D. and Fisher, R.W. (1977) *J. Magn. Reson.*, **28**, 417–426.

Kay, L.E., Nicholson, L.K., Delaglio, F., Bax, A. and Torchia, D.A. (1992) *J. Magn. Reson.*, **97**, 359–375.

Lefèvre, J.-F., Dayie, K.T., Peng, J.W. and Wagner, G. (1996) *Biochemistry*, **35**, 2674–2686.

Lipari, G. and Szabo, A. (1982) *J. Am. Chem. Soc.*, **104**, 4546–4559.

Mack, C. (1967) *Essentials of Statistics for Scientists and Technologists*, Plenum Press, New York, NY, U.S.A.

Marion, D., Ikura, M., Tschudin, R. and Bax, A. (1989) *J. Magn. Reson.*, **85**, 393–399.
Meiboom, S. and Gill, D. (1958) *Rev. Sci. Instrum.*, **29**, 688–691.
Norwood, T.L., Boyd, J., Heritage, J.E., Soffe, N. and Campbell, I. (1990) *J. Magn. Reson.*, **87**, 488–501.
Orekhov, V.Y., Pervushin, K.V. and Arseniev, A.S. (1994) *Eur. J. Biochem.*, **219**, 887–896.
Orekhov, V.Y., Pervushin, K.V., Korzhnev, D.M. and Arseniev, A.S. (1995) *J. Biomol. NMR*, **6**, 113–122.
Otting, G. and Wüthrich, K. (1988) *J. Magn. Reson.*, **76**, 569–574.
Palmer III, A.G., Rance, M. and Wright, P.E. (1991) *J. Am. Chem. Soc.*, **113**, 4371–4380.
Palmer III, A.G., Skelton, N.J., Chazin, W.J., Wright, P.E. and Rance, M. (1992) *Mol. Phys.*, **75**, 699–711.
Peng, J.W., Thanabal, V. and Wagner, G. (1991a) *J. Magn. Reson.*, **94**, 82–100.
Peng, J.W., Thanabal, V. and Wagner, G. (1991b) *J. Magn. Reson.*, **95**, 421–427.
Peng, J.W. and Wagner, G. (1992) *J. Magn. Reson.*, **98**, 308–332.
Peng, J.W. and Wagner, G. (1995) *Biochemistry*, **34**, 16733–16752.
Piotto, M., Saudek, V. and Sklenář, V. (1992) *J. Biomol. NMR*, **2**, 661–665.
Press, W.H., Flannery, B.P., Teukolsky, S.A. and Vetterling, W.T. (1992) *Numerical Recipes in C*, 2nd ed., Cambridge University Press, Cambridge, U.K.
Schleucher, J., Quant, J., Glaser, S.J. and Griesinger, C. (1995) *J. Magn. Reson.*, **A112**, 144–151.
Shaka, A.J., Keeler, J. and Freeman, R. (1983) *J. Magn. Reson.*, **53**, 313–340.
Shaka, A.J. and Keeler, J. (1987) *Prog. NMR Spectrosc.*, **19**, 47–129.
Sklenář, V., Torchia, D. and Bax, A. (1987) *J. Magn. Reson.*, **73**, 375–379.
Szyperski, T., Luginbühl, P., Otting, G., Güntert, P. and Wüthrich, K. (1993) *J. Biomol. NMR*, **3**, 151–164.
Tjandra, N., Feller, S.E., Pastor, R.W. and Bax, A. (1995a) *J. Am. Chem. Soc.*, **117**, 12562–12566.
Tjandra, N., Kuboniwa, H., Ren, H. and Bax, A. (1995b) *Eur. J. Biochem.*, **230**, 1014–1024.
Tjandra, N., Wingfield, P., Stahl, S. and Bax, A. (1996) *J. Biomol. NMR*, **8**, 273–284.
Vold, R.R. and Vold, R.L. (1976) *J. Chem. Phys.*, **64**, 320–332.
Wagner, G. and Wüthrich, K. (1982) *J. Mol. Biol.*, **160**, 343–361.
Wagner, G. (1983) *Q. Rev. Biophys.*, **16**, 1–57.
Wagner, G. (1993) *Curr. Opin. Struct. Biol.*, **3**, 748–754.
Zinn-Justin, S., Roumestand, C., Gilquin, B., Bontems, F., Ménez, A. and Toma, F. (1992) *Biochemistry*, **31**, 11335–11347.